Acta Mechanica 178, 187–197 (2005)
DOI 10.1007/s00707-005-0247-x

Acta Mechanica
Printed in Austria

On the axial flow of an incompressible viscous fluid in a pipe with a porous boundary

M. E. Erdoğan and **C. E. Imrak**, Istanbul, Turkey

Received January 13, 2004; revised November 2, 2004
Published online: August 4, 2005

Summary. Fully developed laminar flow of an incompressible viscous fluid through a porous pipe with suction and injection is considered. An exact solution of the Navier-Stokes equations is given. The solution is in a series form in terms of the modified Bessel functions. The flow properties depend on the cross-Reynolds number, $V.\ a/v$, where V is the suction velocity, a is the radius of the pipe and v is the kinematic viscosity of the fluid. It is found that for large values of the cross-Reynolds number the flow near the region of the suction shows a boundary-layer character. In this region, the velocity varies sharply and the vorticity is concentrated near this region, and in the other parts of the pipe the vorticity does not show an appreciable change. A complete description of the flow is presented by using the graphs of the velocity, the volume flux across a plane normal to the flow and the vorticity.

1 Introduction

An exact solution of the Navier-Stokes equations for flow through a uniformly porous pipe is given. Obtaining the exact solutions of the Navier-Stokes equations is very important for many reasons. They provide a standard for checking the accuracies of many approximate methods such as numerical or empirical. Although computer techniques make the complete integration of the Navier-Stokes equations feasible, the accuracy of the results can be established by a comparison with an exact solution. The exact solution given in this paper is for a flow in a porous pipe. The flow of fluids over boundaries of porous materials has many applications in practice such as boundary-layer control. A simple solution of the Navier-Stokes equations can be obtained for flow over a porous plane boundary at which there is a uniform suction velocity. This solution was found by Griffith and Meredith and was given in [1]. There is no solution of the Navier-Stokes equations for flow over a porous plane boundary at which there is a uniform injection velocity. However, if the porous plane is bounded by side walls, a solution of the Navier-Stokes equations can be found for the injection case [2]. The flow between two parallel porous plates with uniform suction at the upper plate and uniform injection at the lower plate has been considered in [3]. For large values of the suction parameter based on the suction velocity, a characteristic length and the kinematic viscosity of the fluid, the flow near the upper plate has a boundary-layer character. Velocity varies sharply, the vorticity is concentrated near the suction region, and it has nearly a constant value across the channel [3].

The flow in a duct of rectangular cross-section with uniform suction and injection has been examined by Mehta and Jain [4], Sai and Rao [5], and Erdoğan [2]. The velocity, the vorticity and the volume flux depend on the cross-Reynolds number and the aspect ratio. When the

suction parameter approaches zero, the velocity reduces to that for the flow in a duct with rectangular cross-section without porous walls. When the aspect ratio approaches zero, the velocity reduces to that for the flow between two parallel porous walls. The vorticity for the flow in a duct with rectangular cross-section with suction and injection has two components. When the cross-Reynolds number approaches zero, the vorticity reduces to that for the flow in a duct with rectangular cross-section without porous walls. When the aspect ratio approaches zero, the vorticity reduces to that for the flow between two parallel porous plates. For large values of the cross-Reynolds number the variation of the velocity and the vorticity near the region of suction are sharp, and the flow in this region of the duct has a boundary-layer character. In the other regions of the duct, the vorticity has a constant value.

Fully developed non-swirling laminar flow through a porous pipe with injection has been investigated by many authors, and the complete solution to this problem together with a discussion of previous research has been given by Terril and Thomas [6]. Fully developed laminar flow with swirl in a porous pipe with injection has been examined by Terril and Thomas [7]. The velocity for this flow is three-dimensional and varies along the pipe. Recently, three-dimensional flow in a porous channel has been investigated in [8]. The flows considered are only with injection (or suction) along the channel. Therefore, these flows can neither be compared to that of a duct with rectangular cross-section with suction and injection nor to a porous pipe with suction and injection.

In this paper, the flow in a porous pipe with injection and suction is considered. An exact solution of the Navier-Stokes equations is obtained. A complete description of the solution is presented by using the graphs of the velocity, the volume flux across a plane normal to the flow and the vorticity. The velocity and the vorticity depend on only cross-sectional variables; therefore, they do not change along the pipe. The flow considered is affected by a non-dimensional parameter called the cross-Reynolds number. For large values of this parameter near the suction region the flow has a boundary layer character. In this region, the velocity varies sharply and the vorticity is concentrated near this region and does not change appreciably across the pipe.

The velocity distribution for the flow considered is given in a series form in terms of the modified Bessel function of the first kind of order n. When the suction parameter approaches zero, the velocity reduces to that of the flow in a non-porous pipe. For large values of the suction parameter the series for the velocity is slowly convergent. But the values of the velocity can be calculated by using a computer. The variation of the velocity with the nondimensional distance for various values of the suction parameter is illustrated in Fig. 2. This figure shows that the curves which correspond to $\theta = \pi/2$ and $\theta = 3\pi/2$ overlap and the curve at $\theta = 0$ is different from those at $\theta = \pi/2$ and $\theta = 3\pi/2$. The variation of the velocity at $\theta = \pi$ is illustrated in Fig. 3. For large values of the suction parameter near the region of the suction, the velocity distribution shows a boundary layer character. In this region, the velocity varies sharply. Using the boundary-layer analysis an expression for the velocity is given.

The variation of the volume flux across a plane normal to the flow with the suction parameter is illustrated in Fig. 4. When the suction parameter increases the volume flux decreases. The volume flux, for which the suction parameter equals 10, has one half the value of the non-porous pipe. When the suction parameter approaches zero, the volume flux reduces to that of the Poiseuille flow for a non-porous pipe.

The vorticity has two nonzero components which are ω_r and ω_θ, the z-component ω_z is zero, where r, θ, z are the cylindrical polar coordinates. In the case of flow in a non-porous pipe the component ω_r does not occur. For the flow considered here, ω_r vanishes at $\theta = 0$ and $\theta = \pi$. When the suction parameter approaches zero, ω_r reduces to zero. The variation of ω_r with the

suction parameter λ is such that ω_r increases with λ first, has a maximum at about $\lambda = 4$ and then decreases with λ. The other component of the vorticity is ω_θ and when the suction parameter approaches zero, ω_θ reduces to r/a which is the expression for flow in a non-porous pipe. The variations of ω_θ with r/a for various values of λ at $\theta = 0$ and $\theta = \pi$ are illustrated in Fig. 5. It is interesting that there are similarities between the curves in Fig. 5 and those for the flow in a channel of rectangular cross-section. The variation of ω_θ with θ shows that it has a maximum at $\theta = \pi$. For large values of the suction parameter the vorticity is concentrated near the region of the suction. In this region the flow has a boundary-layer character. In other regions of the pipe, the vorticity does not show an appreciable change. For large values of the suction parameter the series that gives ω_θ is slowly convergent. However, the values of ω_θ for various values of λ can be calculated by using a computer. Although by using a method similar to that given in [9] the asymptotic form of the series for vorticity can be obtained as in the case of the velocity, the result is not practical.

2 Basic equations

Fully developed laminar flow of an incompressible viscous fluid in a porous pipe is considered. The flow geometry and the coordinate system are illustrated in Fig. 1. The cylindrical polar coordinates are used. The direction of the suction velocity is taken as the x-axis without loss of generality. The region on the right-hand side of the pipe is the injection region and the region on the left-hand side of the pipe is the suction region. The velocity field is

$$v_r = -V\cos\theta, \quad v_\theta = V\sin\theta, \quad v_z = w(r,\theta), \tag{1}$$

where v_r, v_θ, v_z are the components of the velocity in the cylindrical polar coordinates and $V(>0)$ is the suction velocity. The Navier-Stokes equations are

$$\frac{v_\theta}{r}\frac{\partial v_r}{\partial\theta} - \frac{v_\theta^2}{r} = -\frac{1}{\rho}\frac{\partial p}{\partial r} + \nu\left(-\frac{v_r}{r^2} + \frac{1}{r^2}\frac{\partial^2 v_r}{\partial\theta^2} - \frac{2}{r^2}\frac{\partial v_\theta}{\partial\theta}\right), \tag{2}$$

$$\frac{v_\theta}{r}\frac{\partial v_\theta}{\partial\theta} + \frac{v_r v_\theta}{r} = -\frac{1}{\rho r}\frac{\partial p}{\partial\theta} + \nu\left(-\frac{v_\theta}{r^2} + \frac{1}{r^2}\frac{\partial^2 v_\theta}{\partial\theta^2} + \frac{2}{r^2}\frac{\partial v_r}{\partial\theta}\right), \tag{3}$$

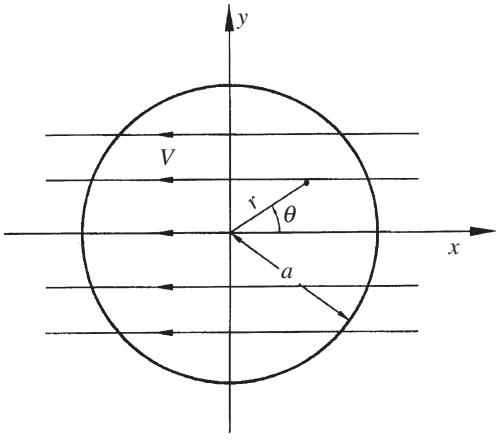

Fig. 1. Flow geometry and coordinate system

$$\upsilon_r \frac{\partial w}{\partial r} + \frac{\upsilon_\theta}{r}\frac{\partial w}{\partial \theta} = -\frac{1}{\rho}\frac{\partial p}{\partial z} + \nu\left(\frac{\partial^2 w}{\partial r^2} + \frac{1}{r}\frac{\partial w}{\partial r} + \frac{1}{r^2}\frac{\partial^2 w}{\partial \theta^2}\right), \tag{4}$$

and the continuity equation is

$$\frac{\partial(r\upsilon_r)}{\partial r} + \frac{\partial \upsilon_\theta}{\partial \theta} = 0, \tag{5}$$

where r, θ, z are the cylindrical polar coordinates, ρ is the density of the fluid, p is the pressure and ν is the kinematic viscosity of the fluid. The continuity Eq. (5) is satisfied identically by Eq. (1). Equations (2) to (4) show that dp/dz is a constant. Equations (2) to (4) reduce to

$$V\left(-\frac{\partial w}{\partial r}\cos\theta + \frac{1}{r}\frac{\partial w}{\partial \theta}\sin\theta\right) = -\frac{1}{\rho}\frac{\partial p}{\partial z} + \nu\left(\frac{\partial^2 w}{\partial r^2} + \frac{1}{r}\frac{\partial w}{\partial r} + \frac{1}{r^2}\frac{\partial^2 w}{\partial \theta^2}\right). \tag{6}$$

Equation (6) is the governing equation, and the boundary condition for the velocity is

$$w(a, \theta) = 0,$$

where a is the radius of the pipe.

3 The velocity distribution

In order to simplify Eq. (6) w can be expressed as

$$w = \frac{1}{\rho V}\frac{dp}{dz} r\cos\theta + e^{-(\lambda r/2a)\cos\theta} F(r, \theta). \tag{7}$$

The first term in Eq. (7) is the inviscid solution and the second term shows the effect of the wall. After inserting Eq. (7) into Eq. (6) one finds

$$\frac{\partial^2 F}{\partial r^2} + \frac{1}{r}\frac{\partial F}{\partial r} + \frac{1}{r^2}\frac{\partial^2 F}{\partial \theta^2} - \frac{\lambda^2}{4}F = 0, \tag{8}$$

where $\lambda = Va/\nu$ is the cross-Reynolds number. The boundary condition becomes

$$F(a, \theta) = \left(-\frac{a}{\rho\nu}\frac{dp}{dz}\cos\theta\right) e^{(\lambda/2)\cos\theta}. \tag{9}$$

The flow in a non-porous pipe is an axisymmetric flow, but the flow in a porous pipe considered in this paper is not an axisymmetric flow. If one replaces θ with $-\theta$ in Eq. (9) the boundary condition does not change. This suggests that $F(r, \theta)$ can be considered as an even function of θ. The solution of Eq. (8) subject to the condition given by Eq. (9) can be obtained by the separation of variables. Since $F(r, \theta)$ is an even function of θ, $F(r, \theta)$ can be expressed in the following form :

$$F(r, \theta) = \sum_{n=0} G_n(r)\cos n\theta, \tag{10}$$

where $G_n(r)$ satisfies the differential equation

$$r^2\frac{d^2 G_n}{dr^2} + r\frac{dG_n}{dr} - \left(\frac{\lambda^2}{4}r^2 + n^2\right)G_n = 0.$$

This differential equation is the Bessel differential equation for the modified Bessel function. Using the uniformity condition at $r = 0$, the solution becomes $A_n I_n(\lambda r/2a)$, where A_n are

constants to be determined by the boundary condition (9), and $I_n(x)$ is the modified Bessel function of the first kind of order n. Equation (10) can be written as

$$F(r,\theta)=\sum_{n=0} A_n I_n(\lambda r/2a)\cos n\theta.$$

Inserting this equation into Eq. (9) and using the identities given in [10]

$$e^{(\lambda/2)\cos\theta}=I_0(\lambda/2)+2\sum_{n=1} I_n(\lambda/2)\cos n\theta \tag{11.1}$$

and

$$e^{(\lambda/2)\cos\theta}\cos\theta=I_1(\lambda/2)+2\sum_{n=1}[I_{n-1}(\lambda/2)+I_{n+1}(\lambda/2)]\cos n\theta, \tag{11.2}$$

one finds

$$A_0=-\frac{a}{\rho V}\frac{dp}{dz}\frac{I_1(\lambda/2)}{I_0(\lambda/2)}, \tag{12}$$

$$A_n=-\frac{a}{\rho V}\frac{dp}{dz}\frac{I_{n-1}(\lambda/2)+I_{n+1}(\lambda/2)}{I_n(\lambda/2)} \quad \text{for } n=1,2,3,\ldots\ . \tag{13}$$

Inserting the values of $A_0, A_1, A_2, \ldots$ into Eq. (10) and then into Eq. (7), the expression for the velocity becomes

$$\frac{w}{-\frac{1}{4\mu}\frac{dp}{dz}a^2}=\frac{4}{\lambda}\left\{-\frac{r}{a}.\cos\theta+e^{-(\lambda r/2a)\cos\theta}\left[\frac{I_1(\lambda/2)}{I_0(\lambda/2)}I_0(\lambda r/2a)\right.\right.$$

$$\left.\left.+\sum_{n=1}\frac{I_{n-1}(\lambda/2)+I_{n+1}(\lambda/2)}{I_n(\lambda/2)}I_n(\lambda r/2a)\cos n\theta\right]\right\}. \tag{14}$$

This solution of the Navier-Stokes equations is exact and valid for all values of λ. For small values of λ, the expression for w can be obtained by Eq. (6) in the following form:

$$\frac{w}{-\frac{1}{4\mu}\frac{dp}{dz}a^2}=1-\frac{r^2}{a^2}-\frac{\lambda}{4}\left(\frac{r}{a}-\frac{r^3}{a^3}\right)\cos\theta+\lambda^2\left[-\frac{1}{32}\left(1-\frac{r^2}{a^2}\right)^2+\frac{1}{48}\left(\frac{r^2}{a^2}-\frac{r^4}{a^4}\right)\cos 2\theta\right]+O(\lambda^3), \tag{15}$$

where $1-(r^2/a^2)$ denotes the velocity distribution for flow in a non-porous pipe.

Using the identities (11.1) and (11.2), it can be shown that the velocity given by Eq. (14) satisfies the condition at $r=a$. The variations of the velocity with r/a for various values of λ at $\theta=0$, $\theta=\pi/2$ and $\theta=3\pi/2$ are illustrated in Fig. 2. It is clearly seen from Fig. 2 that the curves of the velocity at $\theta=\pi/2$ and $\theta=3\pi/2$ overlap and the curve at $\theta=0$ differs from those at $\theta=\pi/2$ and $\theta=3\pi/2$. The variation of the velocity with r/a for various values of λ at $\theta=\pi$ is illustrated in Fig. 3. The variation of the velocity at $\theta=\pi$ is much more different than the others. This is clearly seen from the curves in Fig. 3. For large values of λ near the region of the suction, the variation of the velocity has a boundary-layer character. This effect has also been observed for the flow in a porous duct of rectangular cross-section with suction and injection [2].

In order to analyse the boundary layer near the region of the suction, it is better to write the governing equation (6) in Cartesian coordinates as follows:

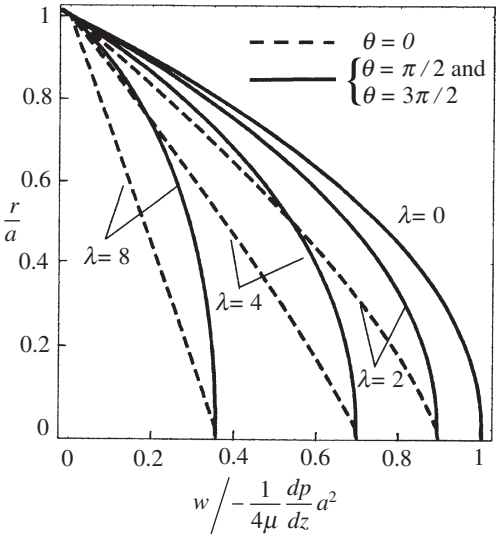

Fig. 2. The variation of $w/-\frac{1}{4\mu}\frac{dp}{dz}a^2$ with r/a for various values of λ. - - - - $\theta = 0$, —— $\theta = \pi/2$ and $\theta = 3\pi/2$

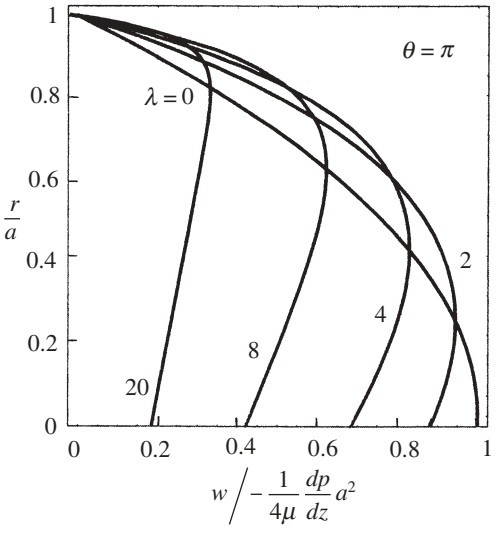

Fig. 3. The variation of $w/-\frac{1}{4/\mu}\frac{dp}{dz}a^2$ with r/a for various values of λ at $\theta = \pi$

$$-V\frac{\partial w}{\partial x} = -\frac{1}{\rho}\frac{dp}{dz} + \nu\left(\frac{\partial^2 w}{\partial x^2} + \frac{\partial^2 w}{\partial y^2}\right). \tag{16}$$

For large values of λ near the region of suction, the variation of the velocity with x is larger than that of y, and then the governing equation in the boundary layer reduces to

$$-V\frac{\partial w}{\partial x} = -\frac{1}{\rho}\frac{dp}{dz} + \nu\frac{\partial^2 w}{\partial x^2}, \tag{17}$$

where w depends on not only x but also y. The solution is

$$w = \frac{1}{\rho V}\frac{dp}{dz}x + A\,e^{-\frac{V}{\nu}x},$$

where A may be a function of y. The first term in the solution corresponds to the inviscid solution for which the vorticity is equal to $-(dp/dz)/\rho V$. By using the boundary condition $w = 0$ at $r = a$, the solution in cylindrical polar coordinates becomes

$$\frac{w}{-\frac{1}{4\mu}\frac{dp}{dz}a^2} = \frac{4}{\lambda}\left[-\frac{r}{a}\cos\theta + e^{\lambda\left(1-\frac{r}{a}\right)\cos\theta}\cos\theta\right]. \tag{18}$$

Equation (18) can be used for large values of λ, and it is valid in the boundary layer near the region of the suction.

4 The volume flux

The volume flux across a plane normal to the flow is given by

$$Q = \int_0^a \int_0^{2\pi} w\, r\, dr\, d\theta.$$

Inserting the expression for w given by Eq. (14) into that for Q and using the identities given in [9]

$$I_n(\alpha) = \frac{1}{2\pi}\int_0^{2\pi} e^{\alpha\cos\theta}\cos n\theta\, d\theta,$$

$$I_n(\alpha) = \frac{(-1)^n}{2\pi}\int_0^{2\pi} e^{-\alpha\cos\theta}\cos n\theta\, d\theta,$$

where α is a parameter and using the identity given in [11]

$$\int_0^a rI_n^2(\lambda r/2a)dr = \frac{a^2}{2}\left[\left(1+\frac{4n^2}{\lambda^2}\right)I_n^2(\lambda/2) - I_n'^2(\lambda/2)\right],$$

one finds

$$\frac{Q}{-\frac{\pi}{8\mu}\frac{dp}{dz}a^4} = \frac{8}{\lambda}\left\{\frac{I_1(\lambda/2)}{I_0(\lambda/2)}\left[I_0^2(\lambda/2) - I_1^2(\lambda/2)\right] + 2\sum_{n=1}(-1)^n\frac{I_n'(\lambda/2)}{I_n(\lambda/2)}\left[\left(1+\frac{4n^2}{\lambda^2}\right)I_n^2(\lambda/2) - I_n'^2(\lambda/2)\right]\right\}, \tag{19}$$

where primes denote differentiation with respect to the arguments. Using the identity given in [9]

$$-I_0(\alpha)I_1(\alpha) + 2\sum_{n=1}(-1)^{n+1}I_n(\alpha)I_n'(\alpha) = 0,$$

Eq. (19) becomes

$$\frac{Q}{-\frac{\pi}{8\mu}\frac{dp}{dz}a^4} = \frac{8}{\lambda}\left[-\frac{I_1^3(\lambda/2)}{I_0(\lambda/2)} + \sum_{n=1}(-1)^{n+1}\frac{I_{n-1}(\lambda/2) + I_{n+1}(\lambda/2)}{I_n(\lambda/2)}I_{n-1}(\lambda/2)I_{n+1}(\lambda/2)\right].$$

When λ approaches zero the volume flux reduces to $\pi(-dp/dz)a^4/8\mu$ which is the volume flux for the flow in a non-porous pipe. The variation of the volume flux across a plane normal to the flow with the cross-Reynolds number is illustrated in Fig. 4. As it is expected, when λ increases

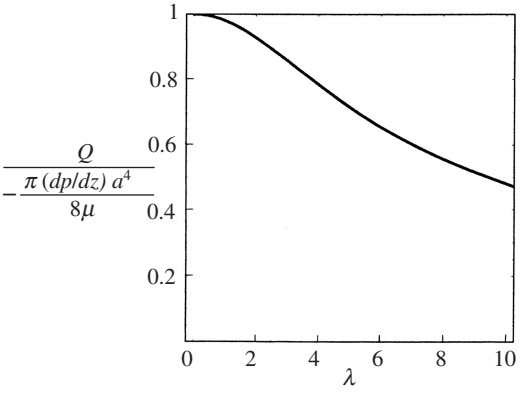

Fig. 4. The variation of $Q/-\frac{\pi}{8\mu}\frac{dp}{dz}a^4$ with λ

the volume flux decreases. The value of the volume flux for $\lambda = 10$ is about half of that for the flow in a non-porous pipe.

5 Vorticity distribution

The components of the vorticity in cylindrical polar coordinates are ω_r, ω_θ and ω_z. The latter component is zero. ω_r andω_θ are given in the following forms:

$$\frac{\omega_r}{-\frac{1}{2\mu}\frac{dp}{dz}a} = \frac{2}{\lambda}\left\{\sin\theta + \frac{\lambda}{2}e^{-(\lambda r/2a)\cos\theta}(\sin\theta)\left[\frac{I_1(\lambda/2)}{I_0(\lambda/2)}I_0(\lambda r/2a) + \sum_{n=1}\frac{I_{n-1}(\lambda/2)+I_{n+1}(\lambda/2)}{I_n(\lambda/2)}I_n(\lambda r/2a)\cos n\theta\right] - \frac{a}{r}e^{-(\lambda r/2a)\cos\theta}\sum_{n=1} n\frac{I_{n-1}(\lambda/2)+I_{n+1}(\lambda/2)}{I_n(\lambda/2)}I_n(\lambda r/2a)\sin\theta\right\}, \tag{20}$$

$$\frac{\omega_\theta}{-\frac{1}{2\mu}\frac{dp}{dz}a} = -\frac{2}{\lambda}\left\{-\cos\theta - \frac{\lambda}{2}e^{-(\lambda r/2a)\cos\theta}(\cos\theta)\left[\frac{I_1(\lambda/2)}{I_0(\lambda/2)}I_0(\lambda r/2a) + \sum_{n=1}\frac{I_{n-1}(\lambda/2)+I_{n+1}(\lambda/2)}{I_n(\lambda/2)}I_n(\lambda r/2a)\cos n\theta\right] + \frac{\lambda}{4}e^{-(\lambda r/2a)\cos\theta}\left[2\frac{I_1(\lambda/2)}{I_0(\lambda/2)}I_1(\lambda r/2a) + \sum_{n=1}\frac{I_{n-1}(\lambda/2)+I_{n+1}(\lambda/2)}{I_n(\lambda/2)}[I_{n-1}(\lambda r/2a)+I_{n+1}(\lambda r/2a)]\cos n\theta\right]\right\}. \tag{21}$$

It is well known that in the case of a non-porous pipe the only nonzero component of the vorticity is ω_θ. ω_r is zero at $r = a$. Indeed, at $r = a$, Eq. (20) becomes

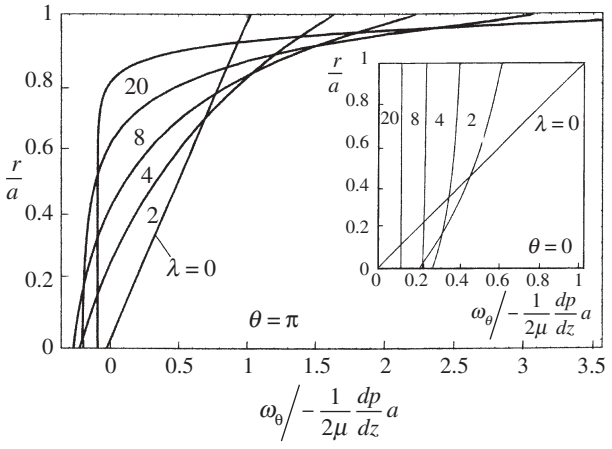

Fig. 5. The variations of $\omega_\theta/-\frac{1}{2\mu}\frac{dp}{dz}a$ with r/a for various values of λ at $\theta=\pi$ and $\theta=0$

$$\frac{\omega_r}{-\frac{1}{2\mu}\frac{dp}{dz}a}=\frac{2}{\lambda}\left\{\sin\theta+\frac{\lambda}{2}(\sin\theta)e^{-\frac{\lambda}{2}\cos\theta}[I_1(\lambda/2)\right.$$

$$+\sum_{n=1}[I_{n-1}(\lambda/2)+I_{n+1}(\lambda/2)]\cos n\theta\Bigg]$$

$$\left.-e^{-\frac{\lambda}{2}\cos\theta}\sum_{n=1}n[I_{n-1}(\lambda/2)+I_{n+1}(\lambda/2)]\sin n\theta\right\}. \tag{22}$$

Using the identities (11.1) and (11.2), Eq. (22) takes the following form:

$$\frac{\omega_r}{-\frac{1}{2\mu}\frac{dp}{dz}a}=\frac{2}{\lambda}\left\{\sin\theta+\frac{\lambda}{2}(\sin\theta)\cos\theta-e^{-\frac{\lambda}{2}\cos\theta}\left[-\frac{\partial}{\partial\theta}\left(e^{-\frac{\lambda}{2}\cos\theta}\cos\theta\right)\right]\right\}.$$

This equation shows that ω_r is zero at $r=a$ for all values of θ. When λ approaches zero, ω_r vanishes. Equation (20) indicates that $\omega_r(r/a,\pi/2)=-\omega_r(r/a,3\pi/2)$. The variation of $\omega_r/(-a\,dp/dz)/2\mu$ with r/a for various values of λ shows that $\omega_r/(-a\,dp/dz)/2\mu$ first increases with λ, reaches a maximum at about $\lambda=4$ and then decreases. The value of $\omega_r/(-a\,dp/dz)/2\mu$ at $r/a=0$ can be calculated by the following equation:

$$\frac{\omega_r(0,\pi/2)}{-\frac{1}{2\mu}\frac{dp}{dz}a}=\frac{2}{\lambda}\left[1+\frac{\lambda}{2}\frac{I_1(\lambda/2)}{I_0(\lambda/2)}-\frac{\lambda}{4}\frac{I_0(\lambda/2)+I_2(\lambda/2)}{I_1(\lambda/2)}\right].$$

The expression of ω_θ is given by Eq. (21). When λ approaches zero, ω_θ takes the following form:

$$\frac{\omega_\theta}{-\frac{1}{2\mu}\frac{dp}{dz}a}=\frac{r}{a},$$

which is the vorticity component in the case of a non-porous pipe and $\omega_\theta=0$ at $r/a=0$. However, in the case of a porous pipe, ω_θ at $r/a=0$ becomes

$$\frac{\omega_\theta}{-\frac{1}{2\mu}\frac{dp}{dz}a}=-\frac{2}{\lambda}\left[-\cos\theta-\frac{\lambda}{2}\frac{I_1(\lambda/2)}{I_0(\lambda/2)}+\frac{\lambda}{4}\frac{I_0(\lambda/2)+I_2(\lambda/2)}{I_1(\lambda/2)}\right],$$

where $\omega_\theta(0,\pi)=-\omega_\theta(0,0)$. For $r=a$, ω_θ can be written as

$$\frac{\omega_\theta}{-\frac{1}{2\mu}\frac{dp}{dz}a} = -\frac{2}{\lambda}\left\{-\cos\theta - \frac{\lambda}{2}e^{-\frac{\lambda}{2}\cos\theta}(\cos\theta)[I_1(\lambda/2) + \sum_{n=1}[I_{n-1}(\lambda/2) + I_{n-1}(\lambda/2)]\cos n\theta\right]$$
$$+\frac{\lambda}{4}e^{-\frac{\lambda}{2}\cos\theta}\left[2\frac{I_1^2(\lambda/2)}{I_0(\lambda/2)} + \sum_{n=1}\frac{[I_{n-1}(\lambda/2) + I_{n+1}(\lambda/2)]^2}{I_n(\lambda/2)}\cos n\theta\right]\Bigg\}.$$

For $\theta = \pi$, using the identity given in [10]

$$I_1(\lambda/2) + \sum_{n=1}(-1)^n[I_{n-1}(\lambda/2) + I_{n+1}(\lambda/2)] = -e^{-\lambda/2},$$

one finds

$$\frac{\omega_\theta}{-\frac{1}{2\mu}\frac{dp}{dz}a} = -\frac{2}{\lambda}\left\{-1 - \frac{\lambda}{2} + \frac{\lambda}{4}e^{\frac{\lambda}{2}}\left[2\frac{I_1^2(\lambda/2)}{I_0(\lambda/2)} + \sum_{n=1}(-1)^n\frac{[I_{n-1}(\lambda/2) + I_{n+1}(\lambda/2)]^2}{I_n(\lambda/2)}\right]\right\}.$$

The variations of $\omega_\theta/(-a\,dp/dz)/2\mu$ with r/a for various values of λ at $\theta = \pi$ and $\theta = 0$ are illustrated in Fig. 5. The curves in Fig. 5 show that for large values of λ the vorticity is concentrated near the region of the suction. This represents a boundary-layer character. However, the variation of $\omega_\theta/(-a\,dp/dz)/2\mu$ at $\theta = 0$ indicates that the flow near the region of the injection does not show a boundary-layer character.

For large values of λ, the numerical calculations of the expressions of the velocity, the volume flux and the vorticity can be realized by using a computer program without difficulty. Although by using a method similar to that given in [9] the asymptotic forms of the series for the velocity, the volume flux and the vorticity can be obtained, they are not practical.

6 Conclusions

The flow considered in this paper is an extension to a porous pipe of the flow through a porous duct of rectangular cross-section with injection and suction. An exact solution of the Navier-Stokes equations is given. It is found that the flow properties such as the velocity, the volume flux across a plane normal to the flow and the vorticity depend on the cross-Reynolds number. These flow properties are expressed in a series form in terms of the modified Bessel functions of the first kind of order n. As the suction parameter approaches zero, they tend to the values for the non-porous pipe. For large values of this parameter a boundary layer occurs near the region of the suction. Using the boundary layer analysis the approximate expression for the velocity is given. In this region the variation of the velocity and the vorticity are sharp. In the other parts of the pipe they do not show an appreciable change. A complete description of the solution is presented by using the graphs of the velocity, the volume flux and the vorticity. The vorticity for flow in a non-porous pipe has only one component which is ω_θ, but for flow in a porous pipe there is also another component which is ω_r. The variation of ω_r shows a maximum at about $\lambda = 4$. The variation of ω_θ with θ has a maximum at $\theta = \pi$. This is due to the boundary layer near the region of the suction, and the vorticity is concentrated near this region.

Acknowledgement

The suggestions of Prof. Dr. N. Aksel and the constructive comments of a referee are gratefully acknowledged.

References

[1] Rosenhead, L. (ed.): Laminar boundary layers. Oxford: Oxford University Press 1963.
[2] Erdoğan, M. E.: The effects of side walls on axial flow in rectangular ducts with suction and injection. Acta Mech. **162**, 157–166 (2003).
[3] Sherman, F. S.: Viscous flow. New York: Mc Graw-Hill 1990.
[4] Mehta, K. N., Jain, R. K.: Laminar hydromagnetic flow in a rectangular channel with porous walls. Proc. Nat. Inst. Sci. India **A28**, 846–856 (1962).
[5] Sai, K. S., Rao, B. N.: Magnetohydrodynamic flow in a rectangular duct with suction and injection. Acta Mech. **140**, 57–64 (2000).
[6] Terrill, R. M., Thomas, P. W.: On laminar flow through a uniform porous pipe. Appl. Sci. Res. **21**, 37–67 (1969).
[7] Terrill, R. M., Thomas, P. W.: Spiral flow in a porous pipe. Phys. Fluids **16**, 386–359 (1973).
[8] Taylor, C. L., Banks, W. H. H., Zetrska, M. A., Drazin, R. G.: Three-dimensional flow in a porous channel. Q. J. Mech. Appl. Math. **44**, 105–133 (1991).
[9] Gold, R. R.: Magnetohydrodynamic pipe flow, part 1. J. Fluid Mech. **13**, 505–512 (1962).
[10] Abramowitz, M., Stegun, I.: Handbook of mathematical functions. New York: Dover 1965.
[11] Carslaw H. S., Jaeger J. C.: Conduction of heat in solids, 2nd ed. Oxford: Oxford University Press 1973.

Authors' address: M. E. Erdoğan and C. E. Imrak, İstanbul Teknik Üniversitesi, Makina Fakültesi, Gümüşsuyu 34439, Istanbul, Turkey (E-mail: imrak@itu.edu.tr)